Filamentation Analysis in Large-Mode-Area Fiber Lasers

Introduction

Fiber lasers have developed rapidly in recent years,[1,2] with output powers above the kilowatt level.[3,4] Along with the increasing output power, nonlinear effects become important and can ultimately limit the power scalability in the fiber. Two well-known nonlinear effects that have limited the output power of fiber lasers are stimulated Brillouin scattering (SBS) and stimulated Raman scattering (SRS). Several methods can be used to increase the SBS threshold, including increasing the signal bandwidth to decrease the Brillouin gain,[5] using new fiber designs to decrease the overlap between acoustic and optics modes,[6] varying the temperature along the cavity,[7,8] and using low-numerical-aperture, large-mode-area (LMA) fibers.[9] Spectral filtering and LMA fibers are also used to mitigate SRS. In LMA fibers, the large mode area serves to decrease the optical intensity, therefore increasing the nonlinear threshold.

While many methods are being investigated to suppress SBS and SRS, other nonlinear effects, such as self-focusing, also have an impact. In 1987 Baldeck *et al.*[10] observed the self-focusing effect in the optical fiber with picosecond laser pulses. Self-focusing can lead to beam-quality degradation through a process called filamentation. The physical nature of filamentation arises from self-focusing through the nonlinear refractive index. When the light intensity is strong enough for self-focusing to occur, the beam in the laser cavity is focused narrower and narrower. As a result, the laser beam is limited in a small region in the center of the core. Thus the corresponding population inversion is depleted in the center of the core, but undepleted in other areas of the core, i.e., spatial hole burning. With spontaneous emission occurring throughout the core, it is easy to generate other lasing beams, finally resulting in filamentation. Filamentation has been studied extensively in semiconductor lasers in the past two decades;[11–13] however, little work has been done in fiber lasers.

In this article, a theoretical model for the filamentation effect in LMA fiber lasers is presented. Solving the paraxial wave equation and population rate equation in three dimensions, an expression for the filament gain is derived using a perturbation method. This expression includes both spatial and temporal characteristics, the filament spacing, and oscillation frequency. The filament gain also depends on the physical parameters of the optical fiber, the nonlinear refractive index, and the pump and signal power. This model can predict the output-power thresholds at which the filamentation will occur for a given set of optical-fiber parameters, in particular the core diameter. A simplified threshold expression is also provided. The results are shown to be consistent with previous experiments.

Theoretical Model and Steady-State Solution

Starting with Maxwell's equation in a dielectric medium, a wave equation is obtained, assuming an optical field of the form $\widetilde{A} = A_s(r,\phi,z,t)e^{i(kz-\omega t)}$ and using the slowly varying envelope approximation to neglect the second derivatives of the time t and axial coordinate z. After considering the gain, loss, nonlinear refractive index, and the coupling of the pump and the signal light in the optical fiber, the optical field of the signal light can be found to satisfy the paraxial wave equation

$$\frac{\partial A_s}{\partial z} + \frac{1}{v_g}\frac{\partial A_s}{\partial t} = \frac{i}{2k_s}\nabla_T^2 A_s + \left[\frac{1}{2}g_s' + i\left(2\gamma_p P_p + \gamma_s P_s\right)\right]A_s, \qquad (1)$$

where A_s is the slowly varying amplitude of the signal light along z and t, v_g is the group velocity, $k_s = n_{\text{eff}}\,k_0$ is the mode propagation constant of the signal light, n_{eff} is the effective index of the refraction, and k_0 is the free-space propagation constant. $\nabla_T^2 = (1/r)(\partial/\partial r) + (\partial^2/\partial r^2) + (1/r^2)(\partial^2/\partial\phi^2)$ is the transverse Laplacian operator, representing diffraction. $g_s' = g_s - \alpha_{\text{cav}}$ is the net gain of the signal light, where $g_s = N_2\sigma_s^e - N_1\sigma_s^a$ is the local gain of the signal light. The energy-level system of the excitation ion is assumed to be a two-level system,[16] where N_2, N_1 are the upper- and lower-state population densities, respectively. σ_j^a, σ_j^e are the absorption and emission cross sections at frequency ω_j with $j = p, s$ representing pump and signal light. To analyze the optical fiber laser, the mirror losses are distributed throughout the cavity, $\alpha_{\text{cav}} = \alpha_{\text{int}} - \ln(R_1R_2)/2L$, where α_{int} is the internal loss, L is the cavity length, and R_1 and R_2 are the reflectivities of the mirrors. For the case of a fiber ampli-

fier, the cavity loss is the same as the internal loss, $\alpha_{cav} = \alpha_{int}$. $\gamma_j = \bar{n}_2 k_0 / A_{\mathrm{eff}_j}$ is the nonlinear parameter at frequency ω_j, $\bar{n}_2$ is the Kerr coefficient, and A_{eff_j} is the effective cross-section area at frequency ω_j. The nonlinear parameter γ_j represents self-focusing in optical fibers, for $\gamma_j > 0$; $P_j = |A_j|^2$ is the optical power in the core at frequency ω_j.

With the assumption of a two-level system, the rate equation of the excited state is given by[16]

$$\frac{\partial N_2}{\partial t} = -\frac{N_2}{\tau} - \left(N_2\sigma_s^e - N_1\sigma_s^a\right)\phi_s - \left(N_2\sigma_p^e - N_1\sigma_p^a\right)\phi_p, \quad (2)$$

where $\phi_j = P_j / \left(A_{\mathrm{eff}_j} h\nu_j\right)$ is the photon flux at the frequency ν_j, τ is the spontaneous lifetime of the excited state, and $N_t = N_1 + N_2$ is the total population density.

Equation (1) is a nonlinear equation without an exact solution. The waveguide mode is first solved in the absence of gain and loss for low-intensity levels (i.e., no nonlinear effects). The solution in the core can be found:[14]

$$\begin{aligned}\widetilde{A} &= A_s \exp\left[i\left(k_s z - \omega_s t\right)\right] \\ &= A_{s_0} J_m\left(p_s r\right)\exp\left(im\phi\right)\exp\left[i\left(k_s z - \omega_s t\right)\right], \end{aligned} \quad (3)$$

where A_{s_0} is a constant, $p_s^2 = n_1^2 k_0^2 - k_s^2$, and n_1 is the refractive index in the core. The index m can take only integer values, with $m = 0$ for the fundamental mode. Therefore, the optical field in Eq. (1) should have the form $A_s = A_{s_1}(z) J_m(p_s r)\exp(im\phi)$. Substituting the Laplacian term with $\nabla_T^2 A_s = -p_s^2 A_s$, Eq. (1) can be rewritten in the steady state as

$$\frac{\partial A_s}{\partial z} = \left[\frac{1}{2}g_s' - \frac{ip_s^2}{2k_s} + i\left(2\gamma_p P_p + \gamma_s P_s\right)\right]A_s. \quad (4)$$

For simplicity, bi-directional pumping is assumed, so the pump power P_p can be regarded as nearly constant along the cavity, which leads to a constant gain along the cavity. When a laser is above threshold, the gain is clamped to the value of cavity loss at threshold. Since the loss is distributed along the cavity in this unfolded cavity model,[13] net gain g_s' is zero and the signal power $P_s = |A_s|^2$ must therefore be independent of $z\left[|A_{s_1}(z)| = A_{s_0}\right]$. Thus, the solution of Eq. (4) has the form $A_s = A_{s_0} J_m(p_s r)\exp(im\phi)\exp(i\Delta k_s z)$, is given by

$$\Delta k_s = \frac{1}{2}g_s' - \frac{ip_s^2}{2k_s} + i\left(2\gamma_p P_p + \gamma_s P_s\right). \quad (5)$$

Equation (5) shows the change for the complex propagation constant due to the gain, loss, nonlinearity, and the waveguide mode.

The modal gain $g_s = \Gamma_s g$ includes the transverse confinement factor $\Gamma_s = A_{\mathrm{effs}} / A_{\mathrm{core}}$ to account for the fact that excited ions are doped only in the core. Substituting the relation $N_1 = N_t - N_2$ into Eq. (2), the upper-state population can be found in the steady state as

$$N_2 = \frac{N_t\left(\dfrac{\sigma_s^a}{\sigma_s^e + \sigma_s^a}\dfrac{P_s}{P_s^{\mathrm{sat}}} + \dfrac{\sigma_p^a}{\sigma_p^e + \sigma_p^a}\dfrac{P_p}{P_p^{\mathrm{sat}}}\right)}{1 + \dfrac{P_s}{P_s^{\mathrm{sat}}} + \dfrac{P_p}{P_p^{\mathrm{sat}}}}, \quad (6)$$

where $P_j = |A_j|^2$, $P_j^{\mathrm{sat}} = \left(A_{\mathrm{eff}_j} h\nu_j\right) / \left[\left(\sigma_j^e + \sigma_j^a\right)\tau\right]$ is defined as saturation power with $j = p, s$. For the case of the fiber laser, with the threshold condition of $g_s = \alpha_{cav}$ and the assumption of constant pump power, the signal power is constant along the z direction in the cavity solved from Eq. (6):

$$\begin{aligned} P_s = \Bigg\{ &-\left(N_t\sigma_s^a + \frac{\alpha_{cav}}{\Gamma_s}\right) \\ &+ \left[\frac{N_t\left(\sigma_p^e\sigma_s^a - \sigma_p^a\sigma_s^e\right)}{\sigma_p^e + \sigma_p^a} + \frac{\alpha_{cav}}{\Gamma_s}\right]\frac{P_p}{P_p^{\mathrm{sat}}}\Bigg\}\frac{\alpha_{cav}P_s^{\mathrm{sat}}}{\Gamma_s}. \end{aligned} \quad (7)$$

Linear Stability Analysis and Filament Gain

The stability of the single-mode solution against nonlinear spatial perturbations must be asserted to determine under what condition beam filamentation will occur. If small perturbations grow with propagation, then the steady-state solution is unstable and the beam can break up under propagation through the fiber. Small perturbations a and n are introduced in the optical field $A_s = \left[\sqrt{P_s} + a(r,\phi,z,t)\exp\left(i\Delta k_s z\right)\right]$ and upper-state population density $N'_2 = N_2 + n(r,\phi,z,t)$. Linearizing Eqs. (1) and (2) in a and n, while using the steady-state solutions, leads to two coupled linear equations:

$$\begin{aligned}\frac{\partial a}{\partial z} + \frac{1}{v_g}\frac{\partial a}{\partial t} = \frac{i}{2k_s}\left(p_s^2 a + \nabla_T^2 a\right) + \frac{1}{2}g_s' a \\ + \frac{1}{2}\Gamma_s n\sqrt{P_s}\left(\sigma_s^e + \sigma_s^a\right) + i\gamma_s P_s\left(a + a^*\right), \end{aligned} \quad (8)$$

$$\begin{aligned} -\tau\frac{\partial n}{\partial t} = n\left(1 + \frac{P_s}{P_s^{\mathrm{sat}}} + \frac{P_p}{P_p^{\mathrm{sat}}}\right) \\ + \left(N_2 - N_t\frac{\sigma_s^a}{\sigma_s^e + \sigma_s^a}\right)\frac{\sqrt{P_s}}{P_s^{\mathrm{sat}}}\left(a + a^*\right). \end{aligned} \quad (9)$$

Due to the cylindrical geometry, the perturbation is assumed to have the form of a Bessel function,

$$a = a_1 J_{k_\phi}(pr)\exp\left[i\left(k_\phi\phi + k_z z - \Omega t\right)\right] + a_2 J_{k_\phi}(pr)\exp\left[-i\left(k_\phi\phi + k_z z - \Omega t\right)\right], \quad (10)$$

$$n = n_0 J_{k_\phi}(pr)\exp\left[i\left(k_\phi\phi + k_z z - \Omega t\right)\right] + n_0^* J_{k_\phi}(pr)\exp\left[-i\left(k_\phi\phi + k_z z - \Omega t\right)\right], \quad (11)$$

where p is a Bessel parameter, k_ϕ has integer value, k_z is the propagation constant of the perturbation, Ω is its oscillation frequency, and n_0, a_1, and a_2 are constants. The two field-perturbation parameters originate from the fact that a represents a complex field, which is determined by two independent variables.[17] The perturbation in population density n is a real number, which can be determined by one variable. Substituting Eqs. (10) and (15) into the coupled equations leads to linear equations about a_1 and a_2^*. In the condition that they have nontrivial solutions, k_z needs to satisfy

$$k_z = \frac{\Omega}{v_g} + i\frac{1}{2}\left[G(1+i\xi) - g_s'\right] \pm \sqrt{\frac{p'^2}{2k_s}\left(\frac{p'^2}{2k_s} - 2\gamma_s P_s\right) - \frac{1}{4}\left[G^2(1+i\xi)^2 + g_s'^2\right]}, \quad (12)$$

where $p'^2 = p^2 - p_s^2$. The factor ξ and the saturated power gain G are defined respectively as

$$\xi = \frac{\Omega\tau}{1 + \dfrac{P_s}{P_s^{\text{sat}}} + \dfrac{P_p}{P_p^{\text{sat}}}}, \quad (13)$$

$$G = \Gamma_s g_s \frac{\dfrac{P_s}{P_s^{\text{sat}}}\left(1 + \dfrac{P_s}{P_s^{\text{sat}}} + \dfrac{P_p}{P_p^{\text{sat}}}\right)}{\left(1 + \dfrac{P_s}{P_s^{\text{sat}}} + \dfrac{P_p}{P_p^{\text{sat}}}\right)^2 + (\Omega\tau)^2}. \quad (14)$$

The steady-state solution is stable provided the perturbation gain (which is the imaginary part of the k_z) is less than the cavity loss, a reflection of the growth of the laser field in the cavity. With the relation $g = -2Im(k_z)$, the perturbation gain can be extracted from Eq. (14), where the factor 2 is added to define the power gain:

$$g = \text{Re}\sqrt{\frac{2p'^2}{k_s}\left(2\gamma_s P_s - \frac{p'^2}{2k_s}\right) + \left[G^2(1+i\xi)^2 + g_s'^2\right]} - (G - g_s'). \quad (15)$$

The negative root from Eq. (12) is selected because the gain needs to be positive for the filamentation to occur. Equation (15) gives a general expression for the filament gain. In a fiber laser, when the population inversion is clamped to the threshold, the net gain g_s' is zero. The filament spacing is defined as $w = \pi/p$, and oscillation frequency $f = |\Omega|/2\pi$.

It is already known that the solution of perturbation must have the form of a Bessel function due to the cylindrical geometry of the fiber. Because the perturbation is also an electromagnetic field, it also needs to satisfy the boundary condition on the interface between the core and cladding, which means for every k_ϕ the Bessel parameter p or filament spacing w has only discrete values. In other words, the perturbation also has mode structure, which is similar to the well-known mode properties of the electromagnetic field in fibers. Equation (15) shows no dependence of k_ϕ to the filament gain, but that does not imply that all the modes can resonate. Mathematically, lower-order modes, especially the fundamental mode of the perturbation, do not have dense enough mode structure for filamentation to occur. Physically, the largest amplitude of the fundamental mode is in the center of the core, where the population is depleted. The amplitudes of higher-order modes are zero at the center and large at the margin where the population is undepleted. Therefore higher-order modes of perturbation are more likely to occur than lower-order modes. The peak-to-peak period of squared higher-order Bessel solutions is approximately equal to π, which accounts for the factor π in the definition of filament spacing.

Spatiotemporal Analysis of Filament Gain in Optical Fiber Lasers

Most high-power fiber lasers are Yb doped, due to high quantum efficiency, high doping density, the absence of excited-state absorption, and a long upper-state lifetime. Therefore the parameters used in this section are for typical Yb-doped fiber lasers and are shown in Table 109.V.

Figure 109.59 shows a 3-D plot of normalized filament gain versus normalized filament spacing and oscillation frequency for the signal peak power P_s = 10 kW and core diameter d_{core} = 100 μm. The figure is symmetric in frequency space; therefore only positive frequency is plotted. To facilitate understanding of Fig. 109.59, normalized gain $g_{\text{norm}} = g/\alpha_{\text{cav}}$ and normalized filament spacing $w_{\text{norm}} = w/a_{\text{core}}$ are used, where a_{core} is the radius of

the fiber core. If perturbation gain is larger than cavity loss ($g_{\text{norm}} > 1$), the filament can grow in the cavity; if filament spacing is less than core radius ($w_{\text{norm}} < 1$), filament can appear in the core. Both of these conditions need to be satisfied for the filament to occur since the gain exists only within the fiber core. In Fig. 109.59 there is a peak in the spatial dimension, which defines the filament spacing at which the perturbation will grow most rapidly, where $g > \alpha_{\text{cav}}$. However, the normalized filament spacing corresponding to the peak region is larger than unity, which means the filament is outside the core, and filamentation cannot occur. In the temporal dimension, the curve is constant with a dip at low frequencies. Since the noise perturbation is dynamic, there is less possibility for the filament to grow statically or in low frequency.

Table 109.V: Parameters for ytterbium-doped optical fiber laser calculations.

Parameter	Value
λ_p	0.976 μm
λ_s	1.053 μm
σ_p^a	2476×10^{-27} m^2
σ_p^e	2483×10^{-27} m^2
σ_s^a	20.65×10^{-27} m^2
σ_s^e	343.0×10^{-27} m^2
N_t	9.4×10^{24} m^{-3}
τ	0.84 ms
Γ_p	0.01
n_{core}	1.46
n_{clad}	1.45562
$\overline{n}_2$	2.6×10^{-20} m^2/W
R_1	1
R_2	0.5
L	0.5 m
α_{int}	0.003 m^{-1}

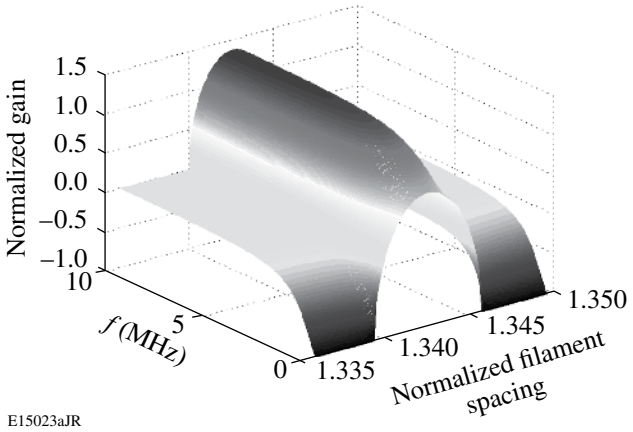

Figure 109.59
Normalized filament gain versus normalized filament spacing and frequency for $d_{\text{core}} = 100$ μm, $P_s = 10$ kW.

In Fig. 109.60, the signal peak power P_s is increased to 10 MW. The gain peak becomes much larger, and the corresponding filament spacing falls into the core. Because both of the thresholds are reached ($g_{\text{norm}} > 1$ and $w_{\text{norm}} < 1$), filamentation can occur. There is no observable feature in the temporal dimension. Thus for signal peak power high above the gain threshold, the temporal modulation of the filamentation can occur at any frequency.

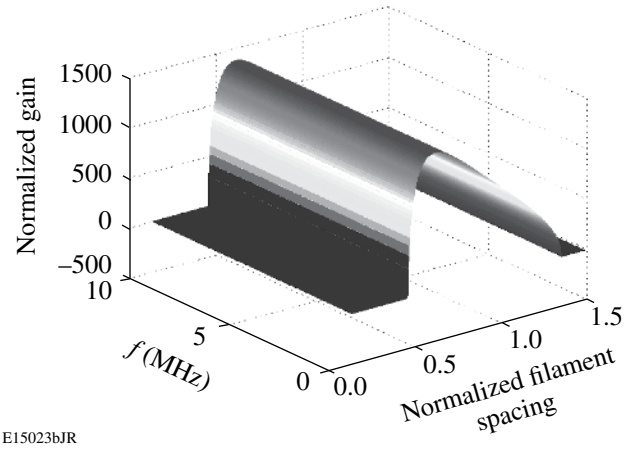

Figure 109.60
Normalized filament gain versus normalized filament spacing and frequency for $d_{\text{core}} = 100$ μm, $P_s = 10$ MW.

Figure 109.61 shows normalized filament spacing and normalized filament gain corresponding to the gain peak as functions of signal peak power for the core diameters ranging from 20 μm to 200 μm, when $f = 10$ GHz. With the increase of the signal peak power, the filament gain peak will move toward the small filament spacing and the filament gain will also increase. This agrees with conventional understanding: the higher the power, the denser the filaments and the larger the possibility for filamentation to occur. From Fig. 109.61 the gain threshold for the filamentation to occur ($g = \alpha_{\text{cav}}$) can also be observed; it is from a magnitude of 100 W to 10 kW for core diameters ranging from 20 μm to 200 μm. The filament spacing threshold, however, is around a few MW, which then determines the filamentation threshold. Self-focusing, and thus filamentation, is determined only by the peak power (highest power) in fiber lasers, regardless of different average powers. Correspondingly, cw (continuous wave) operation is represented by the same curves in Fig. 109.61.

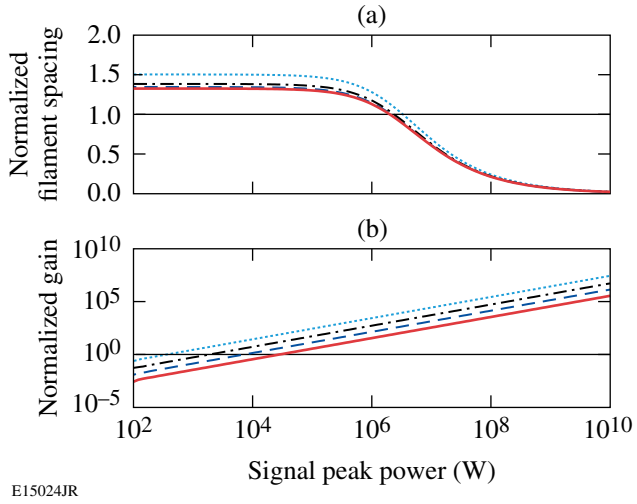

Figure 109.61
(a) Normalized filament spacing and (b) normalized gain as a function of the signal peak power for various core diameters: 20 μm (dotted), 50 μm (dashed–dotted), 100 μm (dashed), and 200 μm (solid) (f = 10 GHz).

The gain peak with respect to the normalized filament spacing can be obtained by solving $\partial g/\partial w = 0$. Correspondingly, the filament spacing and signal peak power have the relation $\pi^2/w^2 = 2\gamma_s k_s P_s + p_s^2$. At spatial threshold $w = a_{\text{core}}$, the spatial threshold power is

$$P_{\text{th}}^{\text{spatial}} = \frac{\left(\pi^2/a_{\text{core}}^2\right) - p_s^2}{2\gamma_s k_s}. \tag{16}$$

At high frequency, saturation gain G and factor ξ can be neglected from Eq. (15), and the filament gain can be simplified at the gain peak as $g = 2\gamma_s P_s$. At gain threshold $g = \alpha_{\text{cav}}$, the gain threshold power is

$$p_{\text{th}}^{\text{gain}} = \frac{\alpha_{\text{cav}}}{2\gamma_s}. \tag{17}$$

Figure 109.62 shows the spatial and gain threshold powers as functions of core diameter. As would be expected from an intensity-dependent process, the gain threshold power increases as the core diameter (and thus mode diameter) increases. Conversely, the spatial threshold power decreases with increasing core diameter. For larger modes, the effects of diffraction and waveguiding are weaker; thus the mode becomes more susceptible to filamentation. For all core diameters below 1000 μm, the spatial threshold dominates.

Figure 109.63 shows the normalized and non-normalized filament gains as functions of the signal peak power for three

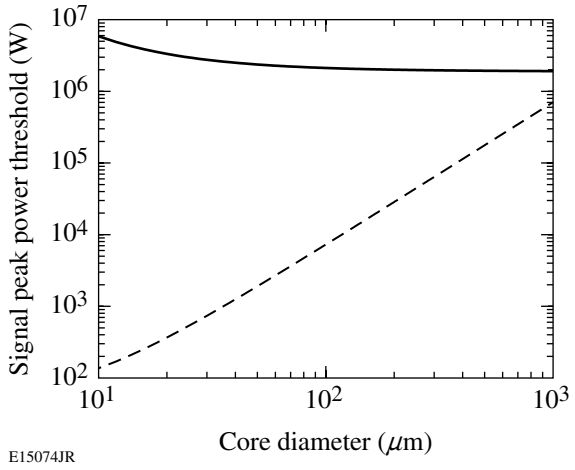

Figure 109.62
Gain threshold power (dashed) and spatial threshold power (solid) as a function of core diameter (f = 10 GHz).

cavity lengths, from 0.5 m to 4 m when d_{core} = 100 μm and f = 10 GHz. It is instructive to see that the normalized gain changes with cavity length since the cavity length relates to the cavity loss in the unfolded cavity model. The non-normalized gain is not affected by the fiber length since it is dependent only on signal peak power. In the laser cavity, light propagates back and forth, and the optical path is effectively infinitely long.

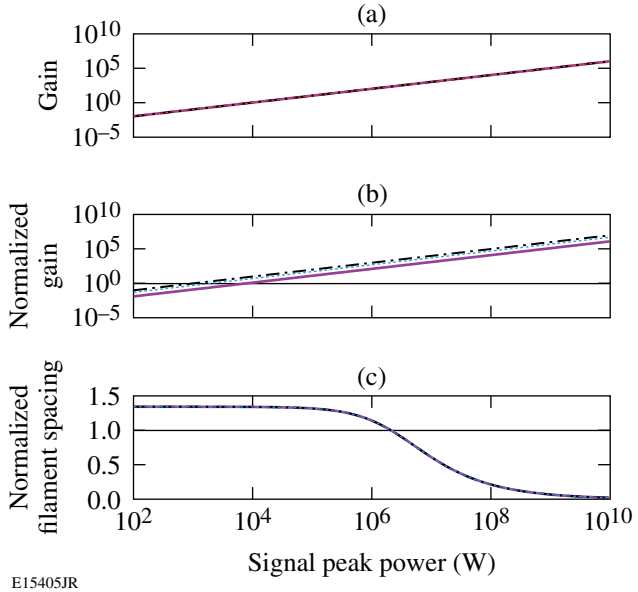

Figure 109.63
(a) Non-normalized filament gain, (b) normalized filament gain, and (c) normalized filament spacing as a function of the signal peak power for three different cavity lengths: 0.5 m (solid), 2 m (dotted), and 4 m (dashed–dotted) (d_{core} = 100 μm, f = 10 GHz).

Thus filamentation can occur as long as the filament gain is larger than cavity loss, and it does not depend on cavity length. Figure 109.63(c) shows a plot of the corresponding normalized filament spacing versus signal peak power. The filament spatial properties do not change with cavity length since they have the same transverse spatial structure. Because spatial threshold determines total threshold here, total threshold is independent of cavity length.

Discussion and Conclusion

Only a single experiment reported self-focusing in multimode optical fibers.[10] In this work, 25-ps pulses were coupled into multimode fiber, and a mode scrambler was used to distribute pulse energy into every mode. The output beam profile was unchanged for pulse energies less than 1 nJ. When the pulse energy was increased beyond 10 nJ, self-focusing occurred. That is to say, the peak power threshold is between 40 W to 400 W. Considering the use of the mode scrambler, the threshold should be much smaller compared to our model, which assumes an unperturbed starting condition of the fundamental mode. Our model gives a gain threshold of around 1 W and a filament spacing threshold of around 0.5 MW. Starting with a set of modes instead of a single mode will lead to a reduction in the filamentation threshold due to the added spatial variations in the initial condition. More recently, an ultrashort Yb-doped fiber laser system was demonstrated with peak power in the fiber of 15 kW (Ref. 4). Since their peak power is still under the filament spacing threshold (~7 MW from our model), no filamentation occurs.

The thresholds of SBS and SRS are around ~20 W and ~1 kW for short-length cw fiber lasers.[7] For short-pulsed fiber lasers, SBS can be neglected for the broadband spectra; the threshold of SRS can be increased to MW using the LMA fibers. Recently, Cheng[18] has reported a 1.56-MW-peak-power laser system using 80-μm-core, Yb-doped LMA fibers. Given the rapid rate of progress in high-peak-power fiber lasers, self-focusing and filamentation will soon become a problem that will need to be addressed in order to retain high-beam-quality output. It is important to note that since these phenomena effectively increase the spatial frequency of the light in the fiber, bend loss will have a beneficial impact on the filamentation threshold.

In summary, an expression for filament power threshold was derived, using a perturbation method, starting from the paraxial wave equation. The spatial and temporal characteristics of the filament gain were analyzed. Two conditions must be satisfied simultaneously for filamentation to occur: filament gain larger than cavity loss and filament spacing less than the core radius. The filamentation also has the mode characteristics of optical fibers, and its threshold is of the order of a few MW.

ACKNOWLEDGMENT

This work was supported by the U.S. Department of Energy Office of Inertial Confinement Fusion under Cooperative Agreement No. DE-FC52-92SF19460, the University of Rochester, and the New York State Energy Research and Development Authority. The support of DOE does not constitute an endorsement by DOE of the views expressed in this article.

REFERENCES

1. B. Ortaç *et al*., Opt. Lett. **28**, 1305 (2003).
2. J. R. Buckley, F. W. Wise, and F. Ö. Ilday, Opt. Lett. **30**, 1888 (2005).
3. Y.-X. Fan *et al*., IEEE Photonics Technol. Lett. **15**, 652 (2003).
4. F. Röser *et al*., Opt. Lett. **30**, 2754 (2005).
5. G. P. Agrawal, *Nonlinear Fiber Optics*, 3rd ed., Optics and Photonics (Academic Press, San Diego, 2001).
6. K. Shiraki, M. Ohashi, and M. Tateda, J. Lightwave Technol. **14**, 549 (1996).
7. J. Toulouse, J. Lightwave Technol. **23**, 3625 (2005).
8. V. I. Kovalev and R. G. Harrison, Opt. Lett. **31**, 161 (2006).
9. C.-H. Liu *et al*., Electron. Lett. **40**, 1471 (2004).
10. P. L. Baldeck, F. Raccah, and R. R. Alfano, Opt. Lett. **12**, 588 (1987).
11. H. Adachihara *et al*., J. Opt. Soc. Am. B **10**, 658 (1993).
12. D. J. Bossert, J. R. Marciante, and M. W. Wright, IEEE Photonics Technol. Lett. **7**, 470 (1995).
13. J. R. Marciante and G. P. Agrawal, IEEE J. Quantum Electron. **33**, 1174 (1997).
14. D. Gloge, Appl. Opt. **10**, 2252 (1971).
15. G. P. Agrawal, *Lightwave Technology: Components and Devices* (Wiley, Hoboken, NJ, 2004).
16. P. C. Becker, N. A. Olsson, and J. R. Simpson, *Erbium-Doped Fiber Amplifiers: Fundamentals and Technology* (Academic Press, San Diego, 1999).
17. C.-J. Chen, P. K. A. Wai, and C. R. Menyuk, Opt. Lett. **20**, 350 (1995).
18. M.-Y. Cheng *et al*., presented at CLEO/QELS 2006, Long Beach, CA, 21–26 May 2006 (Paper CThAA3).